Pattern formation in odd viscoelastic fluids

Carlos Floyd , Aaron R. Dinner , and Suriyanarayanan Vaikuntanathan[*]

The Chicago Center for Theoretical Chemistry, The University of Chicago, Chicago, Illinois 60637, USA;
Department of Chemistry, The University of Chicago, Chicago, Illinois 60637, USA;
and The James Franck Institute, The University of Chicago, Chicago, Illinois 60637, USA

Nonreciprocal interactions fueled by local energy consumption can be found in biological and synthetic active matter at scales where viscoelastic forces are important. Such systems can be described by "odd" viscoelasticity, which assumes fewer material symmetries than traditional theories. Here we study odd viscoelasticity analytically and using lattice Boltzmann simulations. We identify a pattern-forming instability which produces an oscillating array of fluid vortices, and we elucidate which features govern the growth rate, wavelength, and saturation of the vortices. Our observation of pattern formation through odd mechanical response can inform models of biological patterning and guide engineering of odd dynamics in soft active matter systems.

I. INTRODUCTION

A striking feature of nonequilibrium systems is their tendency to undergo spatiotemporal pattern formation [1,2]. Coherent structures such as convective rolls [3], Turing patterns [4], and pulsatile contractions of active gels [5] emerge spontaneously as the active driving in a system overcomes stabilizing dissipative forces. Pattern-forming instabilities are biologically important since, for example, they are utilized by growing organisms for morphogenesis [6]. In many biological examples of soft active matter systems, patterns are driven by the interplay of an active contribution to the local stress [7–9] and a concentration field of chemical regulators [5,10–14]. One can ask whether pattern formation in soft active matter systems can be reached through alternative routes which do not rely on active stresses and gradients of chemical regulators. We show here that pattern formation in a viscoelastic fluid can occur without either of these features, provided that the system displays odd nonequilibrium elastic responses to mechanical deformations.

Odd elasticity, which complements the older theory of odd viscosity [15–21], has been developed by Vitelli and coworkers to describe elastic materials with internal energy-consuming degrees of freedom that do not obey several of the usual symmetries from classical elasticity theory [22–26]. It has recently been reported that certain engineered and even biological systems exhibit odd elasticity: crystals of spinning magnetic colloids [27] and starfish embryos [28], certain active metamaterials [29], and even muscle fibers [30] all transduce energy from an external or chemical drive into nonreciprocal pairwise interactions.

Whereas the predicted phenomenology of odd elastic systems, such as odd elastic waves and negative Poisson ratios [22,23], has been appreciably mapped out, the full implications of odd responses in viscoelastic materials remains to be explored. Some theoretical progress has been made in characterizing the thermodynamics and wave dispersion properties of odd viscoelastic materials [22,24,25]. These works identified novel transport properties and suggested ways that these properties could be experimentally detected; they also proposed that odd dynamics could be important for describing active biological materials like the actomyosin cortex. However, exploring this possibility for complex models which capture the composite nature of biological active matter requires advances in simulation methods to allow for tensorial viscoelastic responses in the hydrodynamic description of multicomponent active viscoelastic fluids.

Here, we report on hydrodynamic simulations of a three-element active viscoelastic fluid using a recently developed extension of the hybrid lattice Boltzmann algorithm which can treat odd viscoelastic forces [31]. Combining these simulations with linear instability analysis, we demonstrate that the interaction of passive viscosity and active odd elasticity allows for the emergence of an oscillating vortex array with a tunable characteristic wavelength and growth rate [Fig. 1(a)]. We additionally show that the initial exponential growth of the vortices saturates if a shear-thickening nonlinearity is included in the dynamics. Our results suggest that such dynamical signatures may be generic to broad classes of odd viscoelastic systems encompassing various microscopic dynamics.

II. ODD VISCOELASTIC FLUID MODEL

Our model for odd viscoelasticity in this paper is an odd Jeffrey fluid. The usual Jeffrey fluid consists of a solvent phase in which a viscoelastic Maxwell material is immersed [32,33], and it has recently been identified as a model with minimally sufficient complexity to quantitatively describe biological materials like the cytoplasm [34,35]. In our case, while we treat
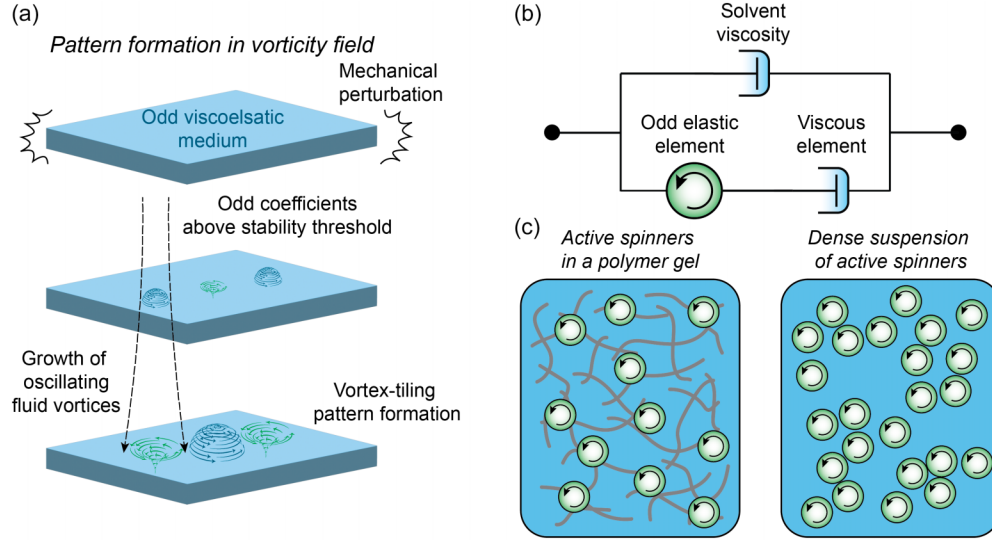
---

*svaikunt@uchicago.edu

FIG. 1. Odd viscoelastic fluids. (a) Schematic illustration of the pattern formation instability observed in odd viscoelastic fluids. (b) A three-element mechanical circuit, comprising a viscous solvent in parallel with an odd Maxwell element, represents a minimal model for an odd composite viscoelastic fluid. (c) Two candidate systems which may display odd viscoelastic phenomenology.

the viscosities of the solvent and viscoelastic phases as scalar, we treat the elastic contribution to the fluid stress using the theory of odd elasticity. The mechanical circuit describing this viscoelastic model is depicted in Fig. 1(b). It can be shown that this model can map directly onto the other three-element viscoelastic fluid models, such as one in which the solvent viscosity acts in series with a Kelvin-Voigt element; see Refs. [32,35]. We expect that an odd Jeffrey fluid could be physically realized in at least two types of systems: one in which active spinners are linked together through a polymer network [36], and one in which attractive interactions between the active spinners cause them to form a dense suspension through viscoelastic phase separation [37,38] [Fig. 1(c)]. A key feature of these systems is that the spinners are not confined to a crystalline order, which would require description as an odd elastic or viscoelastic solid, rather than a fluid [22,27,28,39].

The dynamical equations governing the evolution of the odd Jeffrey fluid are

$$\partial_t \rho = -\partial_i(\rho v_i), \tag{1}$$

$$p = c_s^2 \rho, \tag{2}$$

$$\rho D_t v_i = -\partial_i p + 2\eta_s \partial_k \Psi_{ik} + \partial_k \sigma_{ik}^p + f_i, \tag{3}$$

$$\mathcal{D}_t \sigma_{ij}^p = C_{ijkl} \partial_k v_l - \eta_p^{-1} C_{ijkl} \sigma_{kl}^p + D_p \partial_{kk} \sigma_{ij}^p. \tag{4}$$

Here, ρ is the fluid density, **v** is its velocity, p is its pressure, c_s is the speed of sound in the fluid, η_s is the solvent's dynamic viscosity, $\Psi_{ij} \equiv (\partial_i v_j + \partial_j v_i)/2$ is the symmetric strain rate tensor, and σ^p is the viscoelastic contribution to the stress tensor. The isothermal equation of state, Eq. (2), implies that the fluid is weakly compressible [40]; see Ref. [41] for recent work on the interplay of weak compressibility and odd viscous forces. The term **f** in the Navier-Stokes equation is an optional external force field. **C** is a rank four odd elasticity modulus tensor, η_p is the dynamic viscosity of the

viscoelastic phase (assumed to be scalar here), and D_p is the viscoelastic stress diffusion constant [42]. Odd tensorial viscosity of the viscoelastic phase could be straightforwardly incorporated in this model by generalizing the coefficient $\eta_p^{-1} C_{ijkl}$ in Eq. (4) as a rank four relaxation tensor R_{ijkl} [24]. This would not affect the functional form of the model, so we omit this for simplicity. Further, ∂_t is the partial derivative with respect to time, $D_t \equiv \partial_t + v_k \partial_k$ is the material derivative, and $\mathcal{D}_t X_{ij} \equiv D_t X_{ij} + \Omega_{ik} X_{kj} - X_{ik} \Omega_{kj}$ is the corotational derivative of the tensor **X**, with the vorticity tensor defined as $\Omega_{ij} \equiv (\partial_i v_j - \partial_j v_i)/2$. If the upper convected derivative were used instead of the corotational derivative in Eq. (4), we would have the Oldroyd-B model. In the subsequent linear instability calculation, however, these two derivatives are equivalent because they both reduce to ∂_t to linear order, and our analytical results thus hold for the Oldroyd-B model as well.

In this work we consider an isotropic odd elastic modulus tensor C_{ijkl}, whose form was derived in Ref. [22]:

$$C_{ijkl} = B\delta_{ij}\delta_{kl} + \mu(\delta_{il}\delta_{jk} + \delta_{ik}\delta_{jl} - \delta_{ij}\delta_{kl})$$
$$+ K^o E_{ijkl} - A\epsilon_{ij}\delta_{kl}, \tag{5}$$

where δ_{ij} is the Kronecker delta, ϵ_{ij} is the Levi-Civita tensor, and $E_{ijkl} \equiv (\epsilon_{ik}\delta_{jl} + \epsilon_{il}\delta_{jk} + \epsilon_{jk}\delta_{il} + \epsilon_{jl}\delta_{ik})/2$. The bulk ($B$) and shear ($\mu$) moduli are found in classical elasticity theory, but the modulus A, which transforms a dilatational deformation into torque (but not vice versa), and K^o, which antisymmetrically couples the two shear modes, are the active "odd" moduli. Equation (4) is a phenomenological generalization of a standard Maxwell material to include odd elastic coefficients. It does not correspond to a specific microscopic system, instead serving as a general model to explore the repercussions of nonreciprocity in a composite viscoelastic material. In the Supplemental Material [43], however, we illustrate how one can coarse grain a microscopic "nonreciprocal elastic dumbbell" model to yield continuum equations with emergent odd coefficients like K^o.
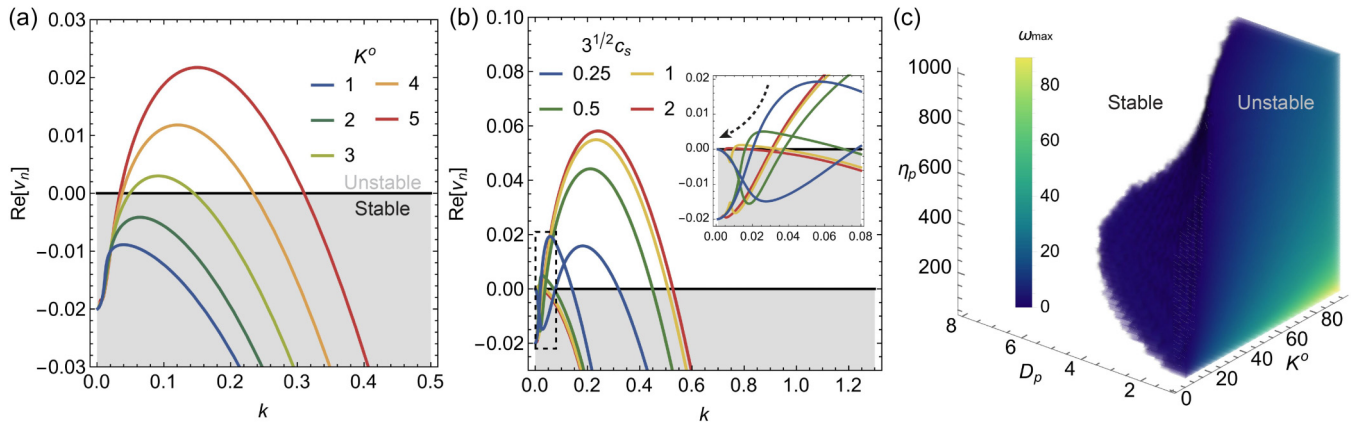
FIG. 2. Dispersion relations. To reduce the number of free parameters, all quantities in this figure are nondimensionalized using the following physical scales: pressure $P = \mu$, length $L = \eta_s/\sqrt{\rho_s \mu}$, and flow speed $V = \sqrt{\mu/\rho_s}$ where ρ_s is the density of the fluid in the uniform state. The default parameters are given in the Supplemental Material [43] . (a) The real part of one of the nine branches ν_n is shown as K^o is varied. (b) Two branches are shown as c_s is varied. The boxed region is blown up and displayed as an inset to allow easier visualization. The dashed arrow indicates that as the system becomes less compressible with increasing c_s, the compressibility-dependent branch of the unstable region decreases to zero. (c) Three-dimensional heatmap of the maximum real part of the growth rate $\omega_{\max}$ in the incompressible limit.

III. RESULTS

The stability of the homogeneous state of the odd Jeffrey fluid is controlled by an intricate balance between stabilizing and destabilizing forces, the relative magnitudes of which depend on the parameters entering Eqs. (1)–(5). In Sec. IIA of the Supplemental Material [43], we derive the dispersion relation $\nu(k)$ for the growth of plane wave perturbations using the ansatz $e^{\nu(k)t}e^{i\mathbf{k}\cdot\mathbf{r}}$ for the pattern forming fields. Linear instabilities occur when $\omega(k) > 0$ for some wave number k, where $\omega(k) \equiv \max_n \mathrm{Re}[\nu_n(k)]$ is the largest of the real parts of nine branches of the dispersion relation $\nu(k)$. The dispersion relation is complicated but reduces to the linear form derived in Ref. [44] in the special case $\eta_s = 0$, $\eta_p \to \infty$, $D_p = 0$, and $A = 0$. Although the stabilizing forces in this composite viscoelastic fluid are more complex than those in a one-component viscoelastic solid as considered in Ref. [22], the intuition provided there of odd work cycles driving active waves also applies to the instabilities found in our model.

We studied how the various parameters control the system's stability by plotting for each parameter the dispersion relation $\omega_{\max} \equiv \max_k \omega(k)$ over a range of parameter values [Fig. 2(a); see Fig. 1 in the Supplemental Material [43] for several other parameters]. Key drivers of the instability include the odd moduli A and K^o: when their values lie outside a threshold set by the remaining parameters, the homogeneous state is unstable. Furthermore, K^o alone is sufficient to cause instability, while A cannot cause instability if $K^o = 0$. The two parameters work cooperatively if their signs agree, such that if $K^o > 0$ then the instability growth rate increases as A increases, but if $K^o < 0$ the growth rate increases as A decreases (Fig. 2 in the Supplemental Material [43]). We also find that the value of the fastest growing wave number $k_{\max} \equiv \mathrm{argmax}_k \omega(k)$ increases with K^o [Fig. 2(a), and Fig. 4(a) in the Supplemental Material [43]] and either increases or decreases with A depending on the relative signs of K^o and A.

The nature of the instability threshold qualitatively changes in the incompressible limit $c_s \to \infty$ (where dilatational deformations disappear, i.e., $\partial_k v_k = 0$). First, as one might expect, the instability no longer depends on the moduli A or B which couple dilatational deformations to, respectively, a torque and an isotropic stress. Additionally, in the compressible case we typically observe two branches of the dispersion relation $\nu_n(k)$ which can take on real positive values for some k. However, in the incompressible limit one of these branches shrinks below zero and remains stable for all k [Fig. 2(b)].

The shear modulus μ, the viscosities η_s and η_p, and the stress diffusion constant D_p have predominantly stabilizing effects, causing $\omega(k)$ to decrease as their values increase [Fig. 2(c), and Fig. 1 in the Supplemental Material [43]]. We note that η_s is a key parameter which suppresses the linear relationship $\omega(k) \propto k$ at large k (Fig. 3 in the Supplemental Material [43]). This allows for a finite $k_{\max}$ and thus a finite length scale of the instability. In previous work [24] η_s was set to zero, precluding the observation of pattern formation since all wavelengths are unstable if $\omega(k) \propto k$.

We next sought to study the growth of the instability in the compressible case using lattice Boltzmann simulations. To simulate an odd Jeffrey fluid, we apply a recently developed implementation of the hybrid lattice Boltzmann algorithm [31]. To excite the instability in simulation we apply a short, periodic, random force $\mathbf{f}(\mathbf{r})$ (see Sec. IIB in the Supplemental Material [43]) and then evolve the system. As a readout of the instability, we use the total absolute vorticity in the system $W \equiv \int |\Omega(\mathbf{r})|d\mathbf{r}$, where $\Omega \equiv \partial_x v_y - \partial_y v_x = 2\Omega_{xy}$. Above the instability threshold, W oscillates and grows exponentially in time [Fig. 3(a)]. If the growth rate is fast enough that W exceeds the value it attained during the initial perturbation in 0.2 s, we conclude that the fluid is unstable. In Fig. 3(b) we show that the conditions of K^o and μ which are predicted to be unstable from the linear instability calculation are matched by those which produce a detected instability in simulation.
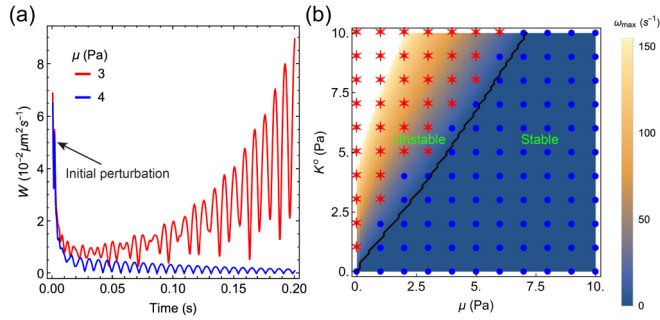
FIG. 3. Numerical validation of instability threshold. (a) For $K^o = 5$ Pa, trajectories of W for two values of μ. See the movies in the Supplemental Material [43] for videos of these simulations. (b) A heatmap of max$\{0, \omega_{max}\}$, with a contour at $\omega_{max} = 0$ drawn in black. When $\omega_{max} > 0$, the homogeneous state of the system is unstable. The symbols are simulation data, with red stars representing a detected instability for that condition and blue circles representing a lack of detected instability.

In Fig. 4(b) of the Supplemental Material [43], we also show that the fastest growing wavelength of the instability matches the characteristic wavelength detected in simulation. As odd active work cycles require more than one spatial dimension [22], we find that under sufficient lateral confinement of the system, the instability is suppressed (Fig. 5 in the Supplemental Material [43]).

The spatial structure of the pattern is a regular periodic array of vortices with alternating handedness. The vorticity at a given point oscillates and grows exponentially in time, as shown in Figs. 4(a) and 4(b), where the vorticity at a point is fit to the functional form

$$\Omega(t) = a \exp(bt) \cos(ct + d). \tag{6}$$

In Fig. 6 of the Supplemental Material [43], we show that the detected growth rate b and oscillation frequency c from simulations match those determined from the real and imaginary parts of the dispersion relationship. We observe both checkerboard and striped patterns which oscillate and grow in time. At later times the patterns are dominantly composed of oscillating stripes of alternating handedness; see Figs. 4(c) and 4(d), and Fig. 7 and movies in the Supplemental Material [43]. The periodic patterns do not travel but instead resemble standing waves. This instability falls in type I_o of the classification of Cross and Hohenberg [1], being periodic in space and oscillatory in time. Although we have focused on the vorticity $\Omega(\mathbf{r})$ as the pattern-forming field, we note that patterning appears for other fields as well, including the divergence, density, and torque, as shown in Fig. 8 in the Supplemental Material [43].

The initial exponential growth of the instability can in principle saturate due to various nonlinearities. The advective term in the Navier-Stokes equation, which is neglected for unsteady Stokes flows at low Reynolds number, is one possibility. We account for this term in our simulations, but we typically observe that the lattice Boltzmann algorithm becomes numerically unstable due to large fluid velocities before saturation from this term occurs. Another possible source is the nonlinear correction to the elastic forces experienced for large deformations, which we neglect here. Treating odd effects in the framework of finite elasticity requires additional theoretical development. Instead, we study here saturation caused by a shear-thickening nonlinearity which can result, for instance, from flocculation of dilatant viscoelastic suspensions like blood [45,46]. We consider a Carreau form [47] $\eta_p(\Psi_{ij}) = \eta_p^0(1 + 2\beta^2\Psi_{ij}\Psi_{ij})^{(n-1)/2}$ which we use in Eq. (4). The parameter β sets the scale at which the shear flow Ψ_{ij} begins to alter the viscosity, and the exponent n determines
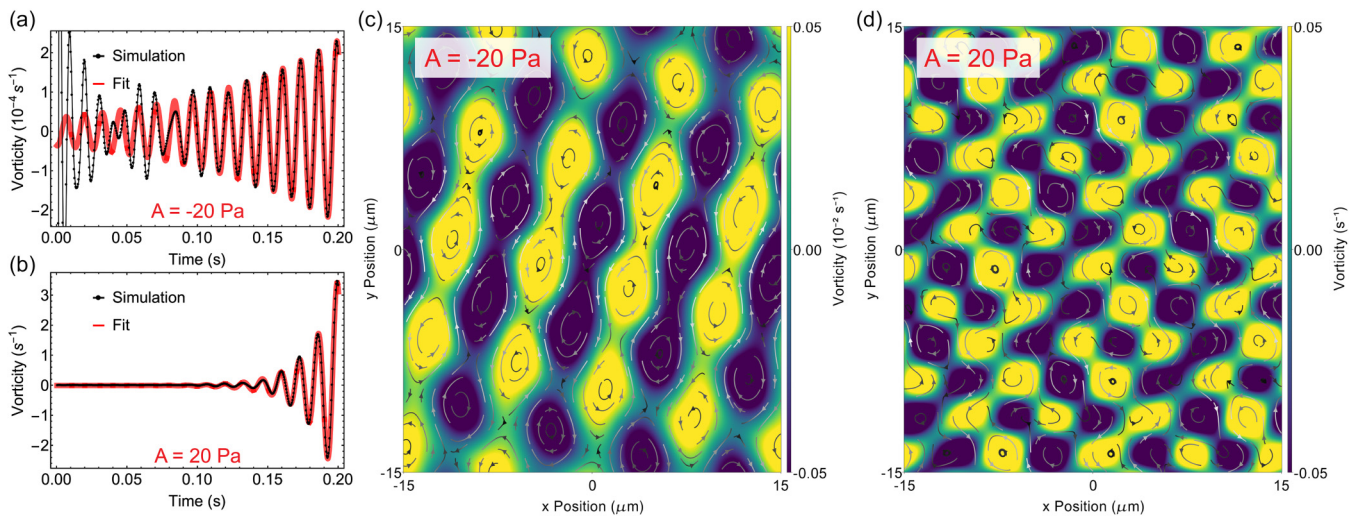

FIG. 4. Simulations of pattern formation. The default parameters are given in the Supplemental Material [43]. (a) The vorticity over time at the point $(-5 \ \mu m, -5 \ \mu m)$ is shown as black symbols for $A = -20$ Pa. The red curve is the fit of Eq. (6) to these data points. The fitting parameters b and c are 9 s^{-1} and 490 s^{-1}. (b) The same as panel (a), but for $A = 20$ Pa. The fitting parameters b and c are 51 s^{-1} and 473 s^{-1}. (c) A simulation snapshot at $t = 0.13$ s for the condition $A = -20$ Pa. Color represents vorticity Ω and the streamlines range from black to white as the represented velocity increases. (d) The same as panel (c), but for $A = 20$ Pa. See movies in the Supplemental Material [43] for videos of these simulations.
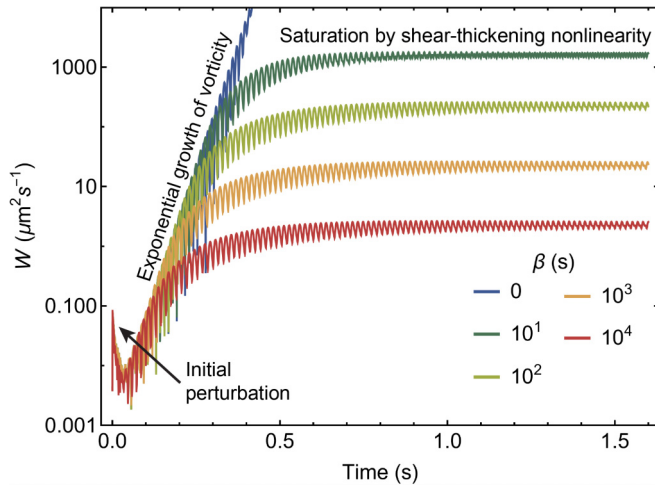
FIG. 5. Saturation of growth by a shear-thickening nonlinearity. The total absolute vorticity W is plotted against time as the parameter β of the Carreau form for shear thickening is varied. The same random seed was used for the initial perturbation in each of these simulations. Here $\eta_p^0 = 0.1$ Pa s and $N_x = N_y = 250$, and the remaining parameters are given in the Supplemental Material [43].

if the system is shear thinning ($n < 1$) or thickening ($n > 1$); here we use $n = 1.5$. In Fig. 5 we display the trajectory $W(t)$ for several values of β, showing that this nonlinearity can significantly tune the flow rate in the pattern forming state of an odd viscoelastic fluid.

IV. CONCLUSION

We have shown that "odd" moduli can provide a mechanism for pattern formation in nonequilibrium viscoelastic fluids. Whereas in typical soft active matter systems pattern formation is driven by active stresses and chemical regulators [5,8–13], here it is driven by active elastic response to mechanical deformations. Given that pattern formation and wave propagation due to active stresses can template developmental processes [6], our discovery of another mechanism for pattern formation may have biological implications. Odd elastic forces could also interact with active stresses and chemical regulators. This may introduce new features to current models of traveling waves, pulsatile motions, and other dynamical patterns known to occur in biological or bioinspired materials like actomyosin sheets [5,10,14,48].

Collectives of rollers [49–52], bacterial suspensions [53,54], as well as both reconstituted and *in vivo* cytoskeletal systems [55,56] exhibit chiral and vortical flows similar

to those reported here. While models for these systems are not currently framed using the theory of odd viscoelasticity, it should be possible to construct emergent, coarse-grained descriptions of their dynamics in terms of odd coefficients. In the Supplemental Material [43] we provide an example of this type of coarse graining for a microscopic "nonreciprocal elastic dumbbell" model; this derivation recapitulates the key coefficient K^o driving instabilities in our phenomenological dynamical equations. A complementary coarse-graining approach to derive continuum odd viscoelasticity was recently presented in Ref. [57]. We note that coarse-graining cytoskseletal systems poses a challenge because the constituent force dipoles are anisotropic, in contrast with the current isotropic model of odd elasticity.

We focused here on the linear instability of an odd Jeffrey fluid, but future work could clarify more of its rheological and dynamical properties. Detectable signatures of odd dynamics should be present even below the instability threshold. To experimentally distinguish an active flow as being due to odd viscoelaticity, we expect that one can exploit the following features: it does not rely on spatial gradients of chemical activators, it comprises strong vortical components, and it requires more than one spatial dimension. We expect that in canonical setups such as Couette or Pouseille flow of a compressible odd Jeffrey fluid, one may find transverse components of the flow analogous to the Hall effect. A recent theoretical study clarifies the expected dynamics experienced by a probe particle immersed in an odd viscoelastic fluid [58]. It would also be worth exploring whether features of pattern formation in other active systems such as screening by substrate friction [59], wavelength selection by confinement [60], and transitions to turbulence [61–63] occur in odd viscoelastic fluids.

[1] M. C. Cross and P. C. Hohenberg, Pattern formation outside of equilibrium, Rev. Mod. Phys. **65**, 851 (1993).

[2] M. Cross and H. Greenside, *Pattern Formation and Dynamics in Nonequilibrium Systems* (Cambridge University Press, Cambridge, UK, 2009).

[3] F. H. Busse, Non-linear properties of thermal convection, Rep. Prog. Phys. **41**, 1929 (1978).

[4] A. M. Turing, The chemical basis of morphogenesis, Bull. Math. Biol. **52**, 153 (1990).

[5] M. F. Staddon, E. M. Munro, and S. Banerjee, Pulsatile contractions and pattern formation in excitable actomyosin cortex, PLoS Comput. Biol. **18**, e1009981 (2022).

[6] P. Gross, K. V. Kumar, and S. W. Grill, How active mechanics and regulatory biochemistry combine to form patterns in development, Annu. Rev. Biophys. **46**, 337 (2017).

[7] M. C. Marchetti, J.-F. Joanny, S. Ramaswamy, T. B. Liverpool, J. Prost, M. Rao, and R. A. Simha, Hydrodynamics of soft active matter, Rev. Mod. Phys. **85**, 1143 (2013).

[8] R. A. Simha and S. Ramaswamy, Hydrodynamic fluctuations and instabilities in ordered suspensions of self-propelled particles, Phys. Rev. Lett. **89**, 058101 (2002).

[9] A. Doostmohammadi, J. Ignés-Mullol, J. M. Yeomans, and F. Sagués, Active nematics, Nat. Commun. **9**, 3246 (2018).

[10] J. S. Bois, F. Jülicher, and S. W. Grill, Pattern formation in active fluids, Phys. Rev. Lett. **106**, 028103 (2011).

[11] K. V. Kumar, J. S. Bois, F. Jülicher, and S. W. Grill, Pulsatory patterns in active fluids, Phys. Rev. Lett. **112**, 208101 (2014).

[12] M. Radszuweit, S. Alonso, H. Engel, and M. Bär, Intracellular mechanochemical waves in an active poroelastic model, Phys. Rev. Lett. **110**, 138102 (2013).

[13] S. Alonso, M. Radszuweit, H. Engel, and M. Bär, Mechanochemical pattern formation in simple models of active viscoelastic fluids and solids, J. Phys. D: Appl. Phys. **50**, 434004 (2017).

[14] C. del Junco, A. Estevez-Torres, and A. Maitra, Front speed and pattern selection of a propagating chemical front in an active fluid, Phys. Rev. E **105**, 014602 (2022).

[15] J. E. Avron, Odd viscosity, J. Stat. Phys. **92**, 543 (1998).

[16] A. Souslov, K. Dasbiswas, M. Fruchart, S. Vaikuntanathan, and V. Vitelli, Topological waves in fluids with odd viscosity, Phys. Rev. Lett. **122**, 128001 (2019).

[17] V. Soni, E. S. Bililign, S. Magkiriadou, S. Sacanna, D. Bartolo, M. J. Shelley, and W. Irvine, The odd free surface flows of a colloidal chiral fluid, Nat. Phys. **15**, 1188 (2019).

[18] M. Han, M. Fruchart, C. Scheibner, S. Vaikuntanathan, J. J. De Pablo, and V. Vitelli, Fluctuating hydrodynamics of chiral active fluids, Nat. Phys. **17**, 1260 (2021).

[19] Z. Liao, M. Han, M. Fruchart, V. Vitelli, and S. Vaikuntanathan, A mechanism for anomalous transport in chiral active liquids, J. Chem. Phys. **151**, 194108 (2019).

[20] C. Hargus, K. Klymko, J. M. Epstein, and K. K. Mandadapu, Time reversal symmetry breaking and odd viscosity in active fluids: Green-Kubo and NEMD results, J. Chem. Phys. **152**, 201102 (2020).

[21] J. M. Epstein and K. K. Mandadapu, Time-reversal symmetry breaking in two-dimensional nonequilibrium viscous fluids, Phys. Rev. E **101**, 052614 (2020).

[22] C. Scheibner, A. Souslov, D. Banerjee, P. Surówka, W. Irvine, and V. Vitelli, Odd elasticity, Nat. Phys. **16**, 475 (2020).

[23] L. Braverman, C. Scheibner, B. VanSaders, and V. Vitelli, Topological defects in solids with odd elasticity, Phys. Rev. Lett. **127**, 268001 (2021).

[24] D. Banerjee, V. Vitelli, F. Jülicher, and P. Surówka, Active viscoelasticity of odd materials, Phys. Rev. Lett. **126**, 138001 (2021).

[25] R. Lier, J. Armas, S. Bo, C. Duclut, F. Jülicher, and P. Surówka, Passive odd viscoelasticity, Phys. Rev. E **105**, 054607 (2022).

[26] M. Fruchart, C. Scheibner, and V. Vitelli, Odd viscosity and odd elasticity, Annu. Rev. Condens. Matter Phys. **14**, 471 (2023).

[27] E. S. Bililign, F. B. Usabiaga, Y. A. Ganan, A. Poncet, V. Soni, S. Magkiriadou, M. J. Shelley, D. Bartolo, and W. Irvine, Motile dislocations knead odd crystals into whorls, Nat. Phys. **18**, 212 (2022).

[28] T. Han Tan, A. Mietke, J. Li, Y. Chen, H. Higinbotham, P. J. Foster, S. Gokhale, J. Dunkel, and N. Fakhri, Odd dynamics of living chiral crystals, Nature (London) **607**, 287 (2022).

[29] Y. Chen, X. Li, C. Scheibner, V. Vitelli, and G. Huang, Realization of active metamaterials with odd micropolar elasticity, Nat. Commun. **12**, 5935 (2021).

[30] S. Shankar and L. Mahadevan, Active muscular hydraulics, bioRxiv 2022.02.20.481216 (2022).

[31] C. Floyd, S. Vaikuntanathan, and A. R. Dinner, Simulating structured fluids with tensorial viscoelasticity, J. Chem. Phys. **158**, 054906 (2023).

[32] R. B. Bird, R. C. Armstrong, and O. Hassager, *Dynamics of Polymeric Liquids. Vol. 1: Fluid Mechanics* (John Wiley and Sons, New York, NY, 1987).

[33] R. G. Larson, *Constitutive Equations for Polymer Melts and Solutions* (Butterworth-Heinemann, Oxford, UK, 2013).

[34] J. Xie, J. Najafi, R. Le Borgne, J.-M. Verbavatz, C. Durieu, J. Sallé, and N. Minc, Contribution of cytoplasm viscoelastic properties to mitotic spindle positioning, Proc. Natl. Acad. Sci. USA **119**, e2115593119 (2022).

[35] J. Najafi, S. Dmitrieff, and N. Minc, Size-and position-dependent cytoplasm viscoelasticity through hydrodynamic interactions with the cell surface, Proc. Natl. Acad. Sci. USA **120**, e2216839120 (2023).

[36] M. P. Howard, R. B. Jadrich, B. A. Lindquist, F. Khabaz, R. T. Bonnecaze, D. J. Milliron, and T. M. Truskett, Structure and phase behavior of polymer-linked colloidal gels, J. Chem. Phys. **151**, 124901 (2019).

[37] H. Tanaka, Viscoelastic phase separation, J. Phys.: Condens. Matter **12**, R207 (2000).

[38] C. P. Royall, S. R. Williams, T. Ohtsuka, and H. Tanaka, Direct observation of a local structural mechanism for dynamic arrest, Nat. Mater. **7**, 556 (2008).

[39] A. P. Petroff, Xiao-Lun Wu, and A. Libchaber, Fast-moving bacteria self-organize into active two-dimensional crystals of rotating cells, Phys. Rev. Lett. **114**, 158102 (2015).

[40] T. Krüger, H. Kusumaatmaja, A. Kuzmin, O. Shardt, G. Silva, and E. M. Viggen, *The Lattice Boltzmann Method: Principles and Practice, Graduate Texts in Physics* (Springer International Publishing, Cham, 2017).

[41] R. Lier, C. Duclut, S. Bo, J. Armas, F. Jülicher, and P. Surówka, Lift force in odd compressible fluids, Phys. Rev. E **108**, L023101 (2023).

[42] P. D. Olmsted, O. Radulescu, and C.-Y. D. Lu, Johnson–Segalman model with a diffusion term in cylindrical couette flow, J. Rheol. **44**, 257 (2000).

[43] See Supplemental Material at http://link.aps.org/supplemental/10.1103/PhysRevResearch.6.033100 for additional figures containing analytical and simulation results, derivation of the linear instability threshold, details of the numerical methods, and a microscopic derivation of the odd viscoelastic equations of motion.

[44] S. Banerjee, M. L. Gardel, and U. S. Schwarz, The actin cytoskeleton as an active adaptive material, Annu. Rev. Condens. Matter Phys. **11**, 421 (2020).

[45] W. H. Boersma, J. Laven, and H. N. Stein, Shear thickening (dilatancy) in concentrated dispersions, AIChE J. **36**, 321 (1990).

[46] T. Bodnár, A. Sequeira, and L. Pirkl, Numerical simulations of blood flow in a stenosed vessel under different flow rates using a generalized Oldroyd-B model, in *AIP Conference Proceedings* (American Institute of Physics, 2009), Vol. 1168, pp. 645–648.

[47] P. J. Carreau, D. C. R. De Kee, and R. P. Chhabra, *Rheology of Polymeric Systems: Principles and Applications* (Carl Hanser Verlag, Munich, 2021).

[48] D. S. Banerjee, A. Munjal, T. Lecuit, and M. Rao, Actomyosin pulsation and flows in an active elastomer with turnover and network remodeling, Nat. Commun. **8**, 1121 (2017).

[49] K. Han, G. Kokot, O. Tovkach, A. Glatz, I. S. Aranson, and A. Snezhko, Emergence of self-organized multivortex states in flocks of active rollers, Proc. Natl. Acad. Sci. USA **117**, 9706 (2020).

[50] K. Han, G. Kokot, S. Das, R. G. Winkler, G. Gompper, and A. Snezhko, Reconfigurable structure and tunable transport in synchronized active spinner materials, Sci. Adv. **6**, eaaz8535 (2020).

[51] B. Zhang, H. Yuan, A. Sokolov, M. Olvera de la Cruz, and A. Snezhko, Polar state reversal in active fluids, Nat. Phys. **18**, 154 (2022).

[52] K. Han, A. Glatz, and A. Snezhko, Globally correlated states and control of vortex lattices in active roller fluids, Phys. Rev. Res. **5**, 023040 (2023).

[53] H. Xu and Y. Wu, Self-enhanced mobility enables vortex pattern formation in living matter, Nature (London) **627**, 553 (2024).

[54] S. Liu, Y. Li, Y. Wang, and Y. Wu, Emergence of large-scale mechanical spiral waves in bacterial living matter, Nat. Phys. **20**, 1015 (2024).

[55] Y. H. Tee, T. Shemesh, V. Thiagarajan, Rizal F. Hariadi, K. L. Anderson, C. Page, N. Volkmann, D. Hanein, S. Sivaramakrishnan, M. M. Kozlov *et al.*, Cellular chirality arising from the self-organization of the actin cytoskeleton, Nat. Cell Biol. **17**, 445 (2015).

[56] V. Schaller, C. Weber, C. Semmrich, E. Frey, and, A. R. Bausch, Polar patterns of driven filaments, Nature (London) **467**, 73 (2010).

[57] P. Matus, R. Lier, and P. Surówka, Molecular modelling of odd viscoelastic fluids, arXiv:2310.15251.

[58] C. Duclut, S. Bo, R. Lier, J. Armas, P. Surówka, and F. Jülicher, Probe particles in odd active viscoelastic fluids: How activity and dissipation determine linear stability, Phys. Rev. E **109**, 044126 (2024).

[59] A. Doostmohammadi, M. F. Adamer, S. P. Thampi, and J. M. Yeomans, Stabilization of active matter by flow-vortex lattices and defect ordering, Nat. Commun. **7**, 10557 (2016).

[60] P. Chandrakar, M. Varghese, S. A. Aghvami, A. Baskaran, Z. Dogic, and G. Duclos, Confinement controls the bend instability of three-dimensional active liquid crystals, Phys. Rev. Lett. **125**, 257801 (2020).

[61] K.-T. Wu, J. B. Hishamunda, D. T. N. Chen, S. J. De Camp, Y.-W. Chang, A. Fernández-Nieves, S. Fraden, and Z. Dogic, Transition from turbulent to coherent flows in confined three-dimensional active fluids, Science **355**, eaal1979 (2017).

[62] S.S. Datta, A.M. Ardekani, P.E. Arratia, A.N. Beris, I. Bischofberger, G.H. McKinley, J.G. Eggers, J.E. Lopez-Aguilar, S.M. Fielding, A. Frishman, M.D. Graham, J.S. Guasto, S.J. Haward, A.Q. Shen, S. Hormozi, A. Morozov, R.J. Poole, V. Shankar, E.S.G. Shaqfeh, H. Stark, V. Steinberg, G. Subramanian, and H.A. Stone, Perspectives on viscoelastic flow instabilities and elastic turbulence, Phys. Rev. Fluids **7**, 080701 (2022).

[63] X. M. de Wit, M. Fruchart, T. Khain, F. Toschi, and V. Vitelli, Pattern formation by turbulent cascades, Nature (London) **627**, 515 (2024).